Nematic fluctuations and semisoft elasticity in swollen liquid-crystal elastomers

Luka Cmok,[1,*] Andrej Petelin,[1,2] and Martin Čopič[1,2]
[1]*Department of Physics, Faculty of Mathematics and Physics, University of Ljubljana, Jadranska 19, SI-1000 Ljubljana, Slovenia*
[2]*Jožef Stefan Institute, Jamova 39, SI-1000 Ljubljana, Slovenia*
(Received 18 November 2014; published 9 April 2015)

Dynamic light scattering (DLS) experiments were performed on stretched sheets of liquid crystal elastomers (LCEs) swollen with a nematic solvent with different swelling ratios. We show that the obtained stress-strain curve and DLS data can still be explained with the concepts of semisoft elasticity. The stress-strain curve shows a typical semisoft response with a threshold strain and a plateau region where stress increases only a little with the applied strain. The width of the plateau decreases with the increase of the swelling ratio because the polymer backbone anisotropy reduces during the swelling. The relaxation rate of thermally excited director fluctuations, however, still shows a typical response, and our measurements indicate the presence of a soft dynamic director-shear mode, as predicted by the theory of semisoft elasticity.

DOI: 10.1103/PhysRevE.91.042502 PACS number(s): 61.30.Vx, 83.80.Va, 78.35.+c

I. INTRODUCTION

Liquid-crystal elastomers (LCEs) [1] show an interesting mechanical response arising from the interplay between the thermal and orientational properties of liquid crystals and the elasticity of the underlying rubbery network. Early experiments performed by Küpfer and Finkelmann [2,3] showed that monodomain nematic elastomers undergo a large spontaneous shape change during the phase transition from the isotropic to the nematic phase. Actuation can also be induced by light [4,5] and to some extent by an electric field, as was first observed by Zentel [6]. An electric field is in general too weak to make any considerable shape change, but in swollen systems with electric fields applied perpendicular to the director a large shape change is observed, which was comprehensively studied by Urayama [7]. The essence of this effect is a so-called *soft elasticity*. It was shown in Ref. [8] that the symmetry-breaking nematic to isotropic phase transition implies the existence of a coupled director-shear soft mode (a Goldstone mode). Because of the zeroing of the shear modulus (relative to the plane containing the nematic director), elastic deformation applied perpendicular to the director, accompanied by a director reorientation, are performed at a zero stress [9,10] in ideal LCEs.

Nowadays, there are several established techniques for fabricating well-aligned monodomain nematic elastomers. The main idea is to freeze-in director orientation during the crosslinking. This can be done either mechanically, by imposing some elastic orienting field during the crosslinking, or to perform alignment in an external orienting electric or magnetic field [11]. The director can be mechanically aligned in the flow in a microfluidic device, as demonstrated in Ref. [12], but the standard technique is to stretch the sample during the second crosslinking step of a so-called two-step crosslinking method [2]. Mechanical alignment is usually much more effective, and samples prepared in this way show a large spontaneous deformation, as opposed to samples aligned by electric fields [13]. The second crosslinking stage makes the elastomeric network anisotropic, so a true isotropic reference state does not exist. Consequently, the elastic response is no longer soft and a large prestretch is needed before the director starts to reorient in the stretching experiment. When deformation in direction x perpendicular to the nematic director z is applied, a nonzero stress is measured with a typical stress-strain relation where initially the stress increases linearly with strain, like in ordinary rubber. Above the threshold strain, extension is accompanied by the director rotation and a shear deformation in the xz plane, and the stress exhibits a soft plateau where stress increases only little with strain. When the rotation of the director is completed, the stress increases again with a similar slope as initially [3,14]. This effect is called *semisoft elasticity*.

One of the most successful models that describes the physics of liquid crystal elastomers is a so-called trace formula developed by the Cambridge group led by Warner and Terentjev [1]. It is a fully nonlinear model that yields an ideally soft response under uniaxial stretching. A semisoft version of the trace formula was also developed. A semisoft response is obtained by adding a small anisotropic correction in the expression for the (soft) free energy, which can be derived for instance from compositional fluctuations [15]. This semisoft model was used extensively in the description of many side-chain systems. One of the main reasons for its widespread use is the simplicity and a low number of parameters of the model. The semisoft model is characterized by only three parameters—the shear modulus μ, the threshold strain for director rotation λ_c, and the chain conformation parameter r—yet it explains all the complexity of the thermomechanical response of LCEs. One of the main features of semisoft elasticity is that exactly at the two threshold strains, that is, at the beginning and at the end of director rotations, the shear modulus for the coupled director-shear deformation in the xz plane (C_5) becomes zero. This is a general, model-independent feature. As pointed out in Ref. [16] and discussed in Ref. [17], any theory including director rotation will lead to zeros in the apparent shear modulus and kinks in the stress-strain curve, and the semisoft version of the trace formula is the most general quadratic free energy that gives the semisoft response. This also explains its success to date in fitting various experimental data.

Yet, some believe that the semisoft model cannot describe systems that were synthesized using the two-step crosslinking

*luka.cmok@fmf.uni-lj.si

method in which large elastic deformations are present during the synthesis [18,19]. Their main argument is that the trace formula is derived from a microscopic picture of Gaussian elasticity in which polymer chains are treated as entropic springs. Furthermore, polymer chain conformation is assumed to be isotropic with a Gaussian distribution in the absence of the nematic field (in the isotropic phase). Because elastomer is stretched during the crosslinking, a true isotropic reference state does not exist and the chain distribution could no longer be Gaussian and there might even be finite extensibility effects associated with the chain elongation. Consequently, the validity of the description based on the microscopic picture of Gaussian elasticity can indeed be questioned.

One of the results of the theory is that it gives a physical meaning to some of the parameters of the model. For instance, the shear constant is $\mu = nk_BT$, where n is the average number of chain segments between crosslinks per unit volume. The shear constants should, therefore, increase with temperature and decrease with swelling (due to the increase of the total volume). In Ref. [18] it was shown that the shear constant of samples prepared according to the two-step crosslinking process increases if the sample is swollen in a nematic solvent. On the other hand, the shear modulus of samples prepared by orienting in electric field before crosslinking does decrease with the increase of the swelling concentration. Authors then conclude that the samples that were synthesized according to the two-step crosslinking method have a non-Gaussian elasticity and that the semisoft description of nematic elasticity does not apply to these materials.

We believe these conclusions are misleading because the scaling of the shear constant with temperature or the swelling concentration does not say anything about the semisoft response of the system. In our previous papers [20–22] we showed that, combined with stress-strain experiments, dynamic light scattering (DLS) is an excellent tool to study the semisoft response. We measured relaxation rates of thermally excited coupled director-shear fluctuations as a function of applied stress in various stretching and scattering geometries. The relaxation rate, as obtained by DLS, is in fact an indirect measure of the shear elastic constant C_5. With a suitable choice of the geometry of the DLS experiment, the zeroing of the shear modulus C_5 at the critical strain can be detected, which was thoroughly explained in Ref. [22]. We showed that at the point of elastic instability, at which the director starts to reorient in the stretching experiment, the relaxation rate of the combined director-shear fluctuation goes to zero, which indicates that it is a soft mode. Furthermore, we showed that samples prepared according to the two-step crosslinking procedure can be well described by the semisoft model, regardless of the crosslinking properties. Samples crosslinked with higher crosslinking densities were stiffer and had a weaker thermomechanical response, but the semisoft response remained conceptually unchanged.

In this paper we show dynamic light scattering and stretching experiments on swollen liquid crystal elastomers prepared by the two-step crosslinking method. We show that the shear constant, contrary to what was observed in Ref. [18], decreases with swelling concentration as expected from the microscopic picture of Gaussian elasticity. The measured elastic response also remains semisoft with a typical stress-strain relation as in the dry samples. With the increase of the concentration of the nematic solvent, the chain conformation parameter r decreases and the width of the plateau in the stretching experiment decreases, which indicates that the coupling between the director and the polymer decreases. Dynamic light scattering reveals the presence of soft modes even at higher swelling concentrations. The results presented in this paper prove that the concepts of semisoft elasticity are valid for a large class of side-chain elastomers prepared according to the two-step crosslinking process.

II. MATERIALS AND METHODS

The samples under study were side-chain LCEs with a siloxane based polymer backbone. They were prepared by the usual two-step crosslinking process with a small stress applied during the second crosslinking stage in the isotropic phase at 80 °C. We used 85 mol% of standard mesogenic moieties M4 [3-but-3-enyl-bezoic acid 4-methoxy-phenylester (TCI)] and 7.5 mol% of a bifunctional crosslinker V1 [1,4-bis-undec-10-enoxy-benzen (TCI)]. Before the swelling, the samples were well aligned, monodomain, and optically transparent. Smaller pieces where cut from one strip of sample that was approximately 5 cm long, 5 mm wide and 300 μm thick. The smaller pieces were measured and weighted before the swelling.

For swelling we used nematic liquid crystal 5CB (Nematel) and 1:1 mixture of organic solvents cyclohexane and toluene (Sigma Aldrich). Toluene was added into the mixture in small steps over a period of 2 hours to prevent rapid swelling which could destroy the polymer network. After complete saturation over 24 hours at ambient conditions the samples were removed from the swelling solution and dried at 60 °C for 24 hours. After the drying process, samples were measured and weighted (see Table I) to obtain the swelling ratio. The weight concentration of the 5CB in the sample was given by

$$X = \frac{m_{5\mathrm{CB}}}{m_{5\mathrm{CB}} + m_{\mathrm{LCE}}}, \tag{1}$$

where $m_{5\mathrm{CB}}$ is the weight of liquid crystal and m_{LCE} is the weight of dry liquid crystal elastomer.

A blank (dry) sample was also made to test if the swelling procedure changes the properties of the sample. This sample was swollen in cyclohexane/toluene mixture with no 5CB content. The blank sample lost 5% of its weight upon drying because of unreacted precursors that were washed out. Dimensions of the dry sample were also changed and the sample was slightly polydomain by appearance. To get the maximum swelling ratio we dip a fresh LCE sample into 5CB and leave the solution for 48 hours at 75 °C so that the LCE and 5CB were in isotropic phase. The obtained sample was fully swollen but, unfortunately, we could not do any stretching and DLS experiments because the Kapton tape that was used to attach the samples for the experiments did not adhere to the sample.

As can be seen in Table I, the swollen samples retain their length in the direction of nematic director (z) but elongate in directions perpendicular to the nematic director. Except for the blank sample, all of the samples became opaque and scattered light strongly, which is an indication of a polydomain.

TABLE I. Dimensions (mm) and mass (g) of the samples before the swelling process, and after they have been swollen with 5CB at a given weight concentration X.

	0.28		0.49		0 (blank)		0.83 (max)	
X	before	after	before	after	before	after	before	after
z	8.9 ± 0.2	8.4 ± 0.2	8.9 ± 0.2	8.7 ± 0.2	8.3 ± 0.2	6.6 ± 0.2	7.4 ± 0.2	8.6 ± 0.2
x	4.9 ± 0.1	7.2 ± 0.2	4.9 ± 0.1	7.5 ± 0.2	5.2 ± 0.1	6.4 ± 0.2	5.5 ± 0.2	12.1 ± 0.3
y	0.37 ± 0.04	0.60 ± 0.07	0.37 ± 0.04	0.60 ± 0.07	0.37 ± 0.04	0.37 ± 0.04	0.35 ± 0.04	0.50 ± 0.07
m	0.022 ± 0.001	0.028 ± 0.001	0.022 ± 0.001	0.040 ± 0.001	0.020 ± 0.001	0.019 ± 0.001	0.014 ± 0.001	0.085 ± 0001

After stretching slightly for about 5% (along the director), the samples became transparent.

For DLS and stress-strain measurements, the samples were placed in a temperature stabilized cell equipped with a micrometer to control the strain and a force gauge to measure the stress on the sample. The light source used in the scattering experiments was a laser operating at $\lambda = 532$ nm. In order to avoid boundary effects from the clamped edges of the samples all of the light scattering experiments were done in the middle of the samples.

The choice of the geometry of the experiment and the scattering vector $\mathbf{q}$ allows for the detection of a particular fluctuation mode $\delta n(\mathbf{q})$. We used the symmetric scattering scheme (Fig. 1), where the incoming scattering angles and the rotation of the sample were chosen so that the scattering vector $\mathbf{q}$ was approximately along the director $\mathbf{n}$, with only a small misalignment ϑ between the director and the wave vector. In such geometry the bend mode polarized in the x direction is observed. As explained in Ref. [22], this is the only possible geometry that allows for a detection of soft modes and should, therefore, be used in the LCE studies. The small misalignment ϑ comes from the fact that wave vectors $\mathbf{k}_i$ and $\mathbf{k}_f$ are not equal in size because of the birefringence of the sample. For small birefringence ($k_i \approx k_f$) the size of the scattering vector is proportional to the scattering angle $q \approx 2k_0 \sin(\theta/2)$, where $k_0 = 2\pi/\lambda$, and $\vartheta \approx 0$ except at very small scattering angles θ.

The scattering data were analyzed with an ALV-6010/160 photon correlator where the normalized intensity correlation function

$$g_2(t) = \frac{\langle I_q(0) I_q(t)\rangle}{\langle I_q(0)\rangle^2} - 1 \tag{2}$$

is calculated from the intensity $I_q(t)$ of scattered light, measured at different times t and different scattering wave numbers q. The intensity has a contribution from a static component, because of the scattering on heterogeneities, and a true dynamic (fluctuating) component which comes from the depolarized scattering from thermally excited nematic fluctuations. A so-called generalized Siegert relation,

$$g_2(t) \approx \alpha^2 g_1^2(t) + 2\alpha(1-\alpha) g_1(t), \tag{3}$$

gives the relation of g_2 to the electric field correlation function $g_1(t)$, where $\alpha = \langle I_{\text{fluct}}\rangle / \langle I_{\text{total}}\rangle$ is the ratio of the dynamic contribution to the detected total intensity. The experimental data were fitted to Eq. (3), where we used the empirical Williams-Watts approximation for the electric field correlation function $g_1(t) \approx \exp(-(t/\tau_{ww})^{\beta})$. The relaxation rate $1/\langle\tau\rangle$ is obtained from the average relaxation time defined as $\langle\tau\rangle = \tau_{ww}\Gamma(1/\beta)/\beta$, where Γ is the gamma function. Our data were fitted well with $\beta \approx 0.5$, which indicates a broad distribution of relaxation times.

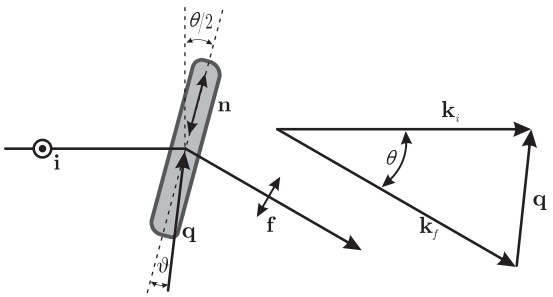

FIG. 1. The geometry of the scattering experiment. The incoming light $\mathbf{k}_i$ was vertically polarized, and horizontally polarized scattered light $\mathbf{k}_f$ was detected and analyzed as a function of scattering angle θ and applied extension λ parallel to $\mathbf{n}$. The scattering vector $\mathbf{q} = \mathbf{k}_i - \mathbf{k}_f$ was approximately parallel to the director (bend mode detection). ϑ is a misalignment between the director and the scattering vector.

III. RESULTS AND DISCUSSION

Light scattering, stress-stain data, and characterization of elastomers are presented in this section. Our experimental techniques allow us to obtain all parameters of the semisoft model. From spontaneous elongation measurements we obtain chain conformation anisotropy parameter $r = (L/L_{\text{iso}})^3$, from stress-strain measurements we obtain the shear constant μ and the threshold strain λ_c, and from light scattering data we obtain the effective viscosity η and the nematic constant K_3. Details on how these parameters are extracted from the measurements can be found in our previous publications [21,22].

First, we show the spontaneous elongation measurements of swollen samples and compare them to the dry sample. The chain conformation parameter $r = (L/L_{\text{iso}})^3$ is obtained from the spontaneous elongation measurements and its temperature dependence is shown in Fig. 2. To obtain these measurements, the sample was hung with the director in the vertical direction and with a small weight attached. Due to a weak polydomain structure of the samples, the weight was needed to make the director align in the vertical direction. We see that the parameter r decreases with the increase of the swelling ratio. This shows that the coupling between the polymer and the director decreases with the inclusion of 5CB molecules. This

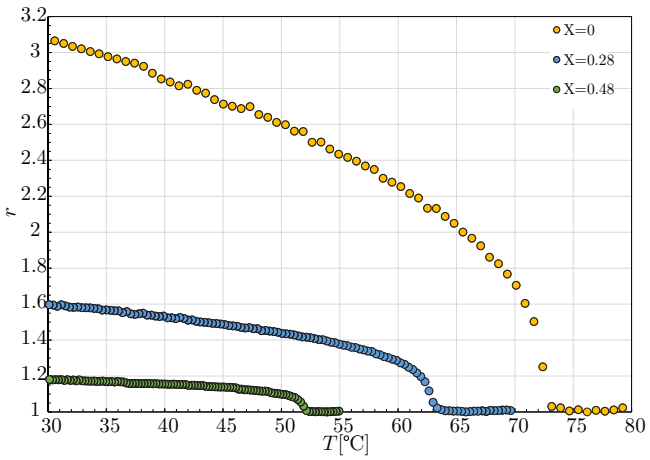

FIG. 2. (Color online) The chain conformation parameter is obtained from the ratio $r = (L/L_{\mathrm{iso}})^3$ of the length of the sample to its reference length. Chain anisotropy r reduces and the nematic to isotropic transition temperature decreases with the increase of the swelling ratio X.

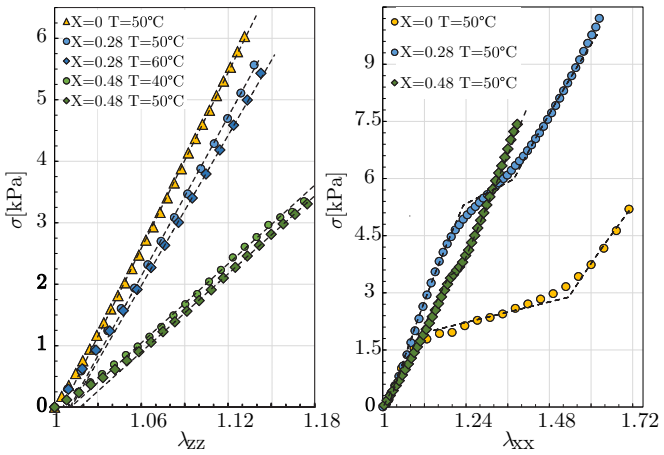

FIG. 3. (Color online) Stress-strain curve for stretching along the director (left) and for the soft geometry (right). Solid lines show fits to the semisoft model from which the shear constants $\mu_\parallel$ and $\mu_\perp$ are obtained.

is probably due to the decrease of the effective density of mesogenic groups that are attached to the polymer. The 5CB molecules are not directly coupled to the polymer, but only couple with the M4 moieties, which effectively reduces the overall coupling between the director and the elasticity of the polymer. The nematic to isotropic (NI) transition temperature also decreases with the weight concentration X, mainly because of a lower phase transition temperature of 5CB, compared to the NI transition temperature of a pure M4 mesogen.

We performed stress-strain experiments in two stretching geometries with deformation applied along the director ($\parallel$) and in the soft geometry where deformation is applied perpendicular to the director ($\perp$), as can be seen in Fig. 3. According to the semisoft model, the nominal stress that is measured in the parallel stretching experiment ($\parallel$) is given by

$$\sigma = \mu\lambda(1-\lambda^{-3}) \approx 3\mu\epsilon, \tag{4}$$

where $\lambda = 1+\epsilon$ is the imposed deformation and ϵ is the strain. The response is linear in a small strain approximation ($\epsilon \ll 1$). Fits to data in Fig. 3 give the shear constant $\mu_\parallel$ (see Table II). When stretch is applied perpendicular to the director we observe a semisoft response with a typical stress-strain curve. According to the semisoft model, the initial slope of the response for $\lambda < \lambda_c$ remains the same as in the parallel stretching geometry, and is given by Eq. (4). Results in Table II, on the other hand, show that the shear constant $\mu_\parallel$ is larger than $\mu_\perp$ by almost a factor of 1.5 for $X = 0$ and $X = 0.28$ and becomes comparable or even smaller at higher swelling ratios at $X = 0.5$. The elastic anisotropy $\mu_\parallel/\mu_\perp$ also depends strongly on the swelling ratio.

In the microscopic picture of Gaussian elasticity, the shear constant decreases with the swelling concentration because of the volume increase and scales as $\mu = \mu_0(V_0/V)^{1/3} = \mu_0(1-X)^{1/3}$, where V_0 is the initial, and V is the final (swollen) volume of the sample, and μ_0 is the shear constant of the unswollen sample. Results, on the other hand, show that the shear constant $\mu_\parallel$ decreases with the increase of the 5CB content, but it does not scale as $(1-X)^{1/3}$. Also, $\mu_\perp$ does not decrease with X and stays, within the experimental error, approximately the same.

The elastic anisotropy and the peculiar dependence on X probably comes from the fact that, in general, nematic order Q also depends on the applied strain, which was neglected in the derivation of Eq. (4). It was found in Ref. [23], both theoretically and experimentally, that the elastic anisotropy shows a rich temperature behavior, with the value $\mu_\parallel/\mu_\perp > 1$ in the nematic phase and even $\mu_\parallel/\mu_\perp < 1$ close to the transition temperature. According to calculation done in Ref. [23] this effect is more pronounced in systems with high chain anisotropy r because of a stronger coupling α between the nematic order Q and the polymer backbone parameter $Q_b = \frac{r-1}{r+2} = \alpha Q$. It was shown that strains applied along the director increase the nematic order Q and extensions perpendicular to

TABLE II. Parameters of the semisoft elastic theory, extracted from the measured stress-strain curve and measurements of the relaxation rate as a function of strain and scattering vector.

X	T (°C)	r	λ_c	$\mu_\parallel$ (10^4 Pa)	$\mu_\perp$ (10^4 Pa)	η (Pa s)	K_3 (10^{-12} N)
0	50	2.7 ± 0.2	1.10 ± 0.02	16 ± 4	10 ± 3		
0.28	50	1.43 ± 0.12	1.16 ± 0.02	14 ± 4	10 ± 3	250 ± 60	9.9 ± 2.4
0.28	60	1.27 ± 0.11	1.16 ± 0.02	14 ± 3		60 ± 15	12 ± 3
0.5	40	1.15 ± 0.10	1.16 ± 0.02	7.3 ± 1.8		150 ± 40	4.1 ± 1.0
0.5	50	1.11 ± 0.09	1.16 ± 0.02	7.1 ± 1.7	12 ± 3	43 ± 10	5.0 ± 1.2

the director induce biaxiality, which in turn gives different slopes in the two stretching experiments. The sample studied in Ref. [23] showed a large spontaneous elongation with $r \approx 4$ at room temperature, so it is comparable to the sample studied in this paper. The elastic anisotropy in their sample was of the order of $\mu_\parallel/\mu_\perp \approx 2$ at lower temperatures ($r > 2$) and close to $\mu_\parallel/\mu_\perp \approx 1$ at higher temperatures ($r < 2$).

The effect of swelling on the elastic anisotropy could, in principle, be addressed within the framework of [23], however, the quality of our data and the lack of measurements of the nematic order parameter Q as a function of X do not allow us to fully study this behavior in detail, so it is left for future studies. We should stress, though, that the elastic anisotropy does not qualitatively change the semisoftness, nor does the swelling, as can be seen from our light scattering data. To probe for the dynamic semisoft response, we measured the relaxation rate of thermally excited director fluctuations as a function of deformation along the director as explained in the previous section. Ideally, we would have stretched perpendicular to the director because this gives a direct indication of the zeroing of the relaxation rate at the threshold λ_c. However, due to the slightly polydomain appearance of the swollen samples, which was more pronounced with the increasing of the swelling ratio, it was not possible to measure in this geometry. By stretching along the director slightly ($\sim$5%), the polydomain texture disappeared and the sample became transparent. In our previous papers we showed that, by stretching along the director, the dynamic soft mode manifests itself in a similar manner. The relaxation rate obtained in this geometry extrapolates to zero at negative strains ($\lambda = 1/\lambda_c$). The relaxation rate, as obtained by DLS, is proportional to the elastic (stress dependent) and nematic restoring torques. These torques, divided by some effective viscosity, give the relaxation rate $1/\tau$. The semisoft model gives an explicit form for the relaxation rate of the bend mode detection scheme that was used in the experiment:

$$\tau^{-1} \approx \frac{\kappa}{\eta}\left(\mu\frac{3\,(r-1)}{r\lambda_c^2}\,(\lambda_c\lambda - 1) + K_3 q^2 + \mu\frac{(r-1)^2}{r^2\lambda_c}\vartheta^2\right), \tag{5}$$

where $\kappa = r^2/((r-1)^2 + r^2)$ is the renormalization constant and η is the effective viscosity. The effective viscosity can be expressed with the Leslie-Ericksen viscous coefficients [22]; at $r \sim 1$ it evaluates to the rotational viscosity of the director $\eta \sim \gamma_1$. The magnitude of the scattering vector is denoted by q, and ϑ is the angle between the director and the scattering vector. The last term in Eq. (5) is a correction which comes from a slight misalignment of the director and the orientation of the scattering vector in the bend-mode detection scheme as explained in the previous section. For typical values of the parameters in DLS experiment with $q = 2k_0 \sin(\theta/2) = 10^{-7}$ m^{-1} and refractive indices $n_o = 1.5$ and $n_e = 1.6$ we get $\vartheta \approx 0.08$, so we can neglect it. The above expression states that at $\lambda = 1/\lambda_c$ and at a long wavelength limit at $q = 0$ the relaxation rate τ^{-1} goes to zero. Therefore, extrapolation of the results to negative strains also reveals the existence of the soft mode. Since the threshold strain is of the order of $\lambda_c \approx 1.1$ and is approximately the same at $X = 0.28$ and $X = 0.5$ and independent of temperature, the extrapolated data should meet in the same point at $\lambda \approx 0.9$. Our measurements in Fig. 4 indeed show that the relaxation rate increases with strain and the extrapolated data have a common origin at around $\lambda \approx 0.9$. This is an indication of the presence of the dynamic soft mode and it supports the validity of the concepts of semisoft elasticity in swollen samples. We should note that for a relaxed (unstretched) state at $\lambda = 1$ and at strains below $\lambda = 1.05$ the samples were not transparent enough and only a small dynamic component was detected in the scattered light. This made the analysis of the results inaccurate and some of the data points were excluded from the Fig. 4. Above $\lambda = 1.05$ the sample cleared out and the scattering was mostly from the nematic fluctuations with a much lower static component in the detected signal. Data were fitted with Eq. (5), where r was determined from Fig. 2 and μ and λ_c were determined from the stress-strain measurements. From fits to the data we obtain the effective rotational viscosity η. The effective viscosity decreases with temperature, due to the Arrhenius activation scheme [21], but also decreases with the swelling concentration, as can be seen from Table II.

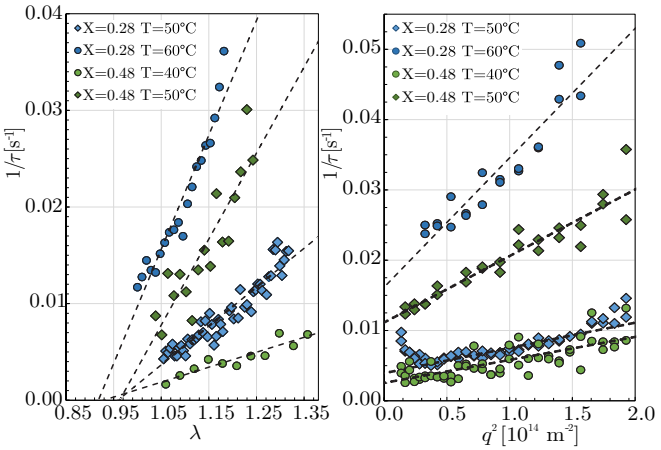

FIG. 4. (Color online) Bend mode relaxation rate as a function of imposed extension λ along the director measured at $q = 10^7$ m^{-1} (left), and as a function of wave vector q at a fixed deformation $\lambda = 1.1$. The relaxation rate increases with λ, and extrapolation of results to negative strain reveals the existence of a dynamic soft mode. The relaxation rate is also proportional to the square of the wave vector, as expected.

Data in Fig. 4 also shows the dependence of the relaxation rate as a function of scattering vector q. We performed light scattering at different scattering vectors q on the slightly stretched samples. The results were obtained at approximately $\lambda = 1.1$ strain to make sure that the sample was clear and that the scattering signal had a large dynamic contribution. In dry samples with high r this would in general give a large elastic contribution to the restoring torque for the director relaxation and it would be difficult to see the q^2 dependence. For the samples studied here, however, the anisotropy was low $r < 1.4$ and the shear constant μ was small, so the nematic contribution scaling as $K_3 q^2$ is of the same order as the first term in Eq. (5), even at $\lambda = 1.1$. The slight increase of the relaxation rate at small q for the $X = 0.28$ sample at $T = 50\,^\circ$C is due to the ϑ term in Eq. (5). At smaller q values the misalignment ϑ

becomes more significant, especially in samples with higher chain conformation r. From fits to the data in Fig. 4 we measured the Frank elastic constant K_3 and find it to be in the expected range (see Table II and [20] for comparison to K_3 measured in dry samples).

IV. CONCLUSIONS

In this paper we analyzed the semisoft response of a side-chain nematic elastomer that was swollen with 5CB. Our dynamic light scattering data and the stress-strain analysis reveals that the semisoft response of swollen LCEs, compared to the dry samples, remains qualitatively unchanged even at high swelling ratios. We observed that the shear constant $\mu_\perp$ decreases with the swelling ratio X and increases with temperature, but shear constant $\mu_\parallel$ remains unchanged. The phase transition temperature decreases with the increase of the swelling ratio because of a low nematic to isotropic transition temperature of the 5CB. Spontaneous elongation measurements show that the chain anisotropy parameter r decreases with the swelling ratio because of a reduced coupling between the director and the elasticity of the polymer. One of the most important observations is that of the existence of the dynamic soft mode in LCEs. We performed dynamic light scattering as a function of strain applied along the director. The extrapolation of the results to negative strains $1/\lambda_c$ reveals that the relaxation rate of the thermally excited director fluctuations goes to zero at the critical strain, as predicted by the theory. We also measured the Frank elastic constant K_3 and found that it is within the expected range.

Based on the results presented in this and our previous papers we can conclude that the semisoft model is much more general than one would expect from its microscopic picture. If one forgets about the microscopic origin of the elastic constants that appear in the model and sets them as a constant yet to be determined from the experiment, a very good agreement with experimental data can be found. In the future it might be interesting to test how the magnitude of the strain imposed during the second crosslinking step affects the semisoft behavior. It could be that the samples in Ref. [18] were stretched beyond what was really necessary to obtain a good director alignment, hence making them non-Gaussian. However, to draw any conclusions regarding the validity of the semisoft description for samples analyzed in Ref. [18], an analysis similar to that presented in this paper should be made. The semisoft elasticity is characterized by the zeroing of the relaxation rate of the nematic fluctuations, accompanied by the zeroing of the shear modulus C_5 at the critical strain λ_c. None of the side-chain systems crosslinked with the usual two-step crosslinking method we have tested so far have shown any considerable deviations from the semisoft response, and we have observed the zeroing of the relaxation rate at the threshold strain in all of the samples. Furthermore, we were able to fit (with a reasonable accuracy) all our data to the simple semisoft trace formula developed by Warner and Terentjev. This supports the validity of the concepts of soft elasticity and that the semisoft model can be used to describe a large class of side-chain liquid-crystal elastomers synthesized according to the two-step crosslinking method.

ACKNOWLEDGMENTS

This research has been supported by Slovenian Research Agency (Grant No. J1-4307).

[1] M. Warner and E. M. Terentjev, *Liquid Crystal Elastomers* (Oxford University Press, New York, 2007).
[2] J. Küpfer and H. Finkelmann, Makromol. Chem., Rapid Commun. **12**, 717 (1991).
[3] J. Küpfer and H. Finkelmann, Macromol. Chem. Phys. **195**, 1353 (1994).
[4] H. Finkelmann, E. Nishikawa, G. G. Pereira, and M. Warner, Phys. Rev. Lett. **87**, 015501 (2001).
[5] P. M. Hogan, A. R. Tajbakhsh, and E. M. Terentjev, Phys. Rev. E **65**, 041720 (2002).
[6] R. Zentel, Liq. Cryst. **1**, 589 (1986).
[7] K. Urayama, H. Kondo, Y. O. Arai, and T. Takigawa, Phys. Rev. E **71**, 051713 (2005).
[8] L. Golubović and T. C. Lubensky, Phys. Rev. Lett. **63**, 1082 (1989).
[9] M. Warner, P. Bladon, and E. M. Terentjev, J. Phys. II France **4**, 93 (1994).
[10] P. D. Olmsted, J. Phys. II France **4**, 2215 (1994).
[11] A. Buguin, M.-H. Li, P. Silberzan, B. Ladoux, and P. Keller, J. Am. Chem. Soc. **128**, 1088 (2006).
[12] C. Ohm, C. Serra, and R. Zentel, Adv. Mater. **21**, 4859 (2009).
[13] M. Brehmer, R. Zentel, G. Wagenblast, and K. Siemensmeyer, Macromol. Chem. Phys. **195**, 1891 (1994).
[14] S. M. Clarke, A. Hotta, A. R. Tajbakhsh, and E. M. Terentjev, Phys. Rev. E **64**, 061702 (2001).
[15] G. C. Verwey and M. Warner, Macromolecules **30**, 4189 (1997).
[16] J. S. Biggins, E. M. Terentjev, and M. Warner, Phys. Rev. E **78**, 041704 (2008).
[17] A. DeSimone and L. Teresi, Eur. Phys. J. E **29**, 191 (2009).
[18] D. Rogez, F. Brömmel, H. Finkelmann, and P. Martinoty, Macromol. Chem. Phys. **212**, 2667 (2011).
[19] D. Rogez and P. Martinoty, Eur. Phys. J. E **34**, 1 (2011).
[20] A. Petelin and M. Čopič, Phys. Rev. Lett. **103**, 077801 (2009).
[21] A. Petelin and M. Čopič, Phys. Rev. E **82**, 011703 (2010).
[22] A. Petelin and M. Čopič, Phys. Rev. E **87**, 062509 (2013).
[23] H. Finkelmann, A. Greve, and M. Warner, Eur. Phys. J. E **5**, 281 (2001).